Conf-911213--22

PNL-SA--19773

DE92 007182

FIBER-OPTIC INTERFEROMETRIC SENSOR FOR GAS FLOW MEASUREMENTS

W. R. Kaminski
J. W. Griffin
J. M. Bates

December 1991

Presented at the
1991 ASME Winter Annual Meeting
December 2, 1991
Atlanta, Georgia

Work supported by
the U.S. Department of Energy
under Contract DE-AC06-76RLO 1830

Pacific Northwest Laboratory
Richland, Washington 99352

DISCLAIMER

FIBER-OPTIC INTERFEROMETRIC SENSOR FOR GAS FLOW MEASUREMENTS[1]

W. R. KAMINSKI
Associate Professor and Coordinator
Mechanical Engineering Technology
Central Washington University
Ellensburg, Washington 98926

J. W. GRIFFIN
Automation and Measurement Sciences Department
Pacific Northwest Laboratory
Richland, Washington 99352

J. M. BATES
Analytic Sciences Department
Pacific Northwest Laboratory
Richland, Washington 99352

ABSTRACT

This paper presents the results of an investigation to determine the feasibility of a novel approach to measuring gas flow in a pipe. An optical fiber is stretched across a pipe and serves as a sensor which is based upon the well-established principle of vortex shedding of a cylinder in cross-flow. The resulting time varying optical signal produces a frequency component proportional to the average velocity in the pipe which is in turn proportional to volumetric flow. A Mach-Zehnder interferometer is used to enhance the accuracy of the vortex shedding frequency signal. The analytical and experimental effort discussed herein shows that the concept is feasible and holds promise for a sensitive and accurate flow measuring technique.

---

[1] By acceptance of this article, the publisher and/or recipient acknowledges the U.S. Government's right to retain a non-exclusive, royalty-free license in and to any copyright covering this paper.

This research was supported by the Northwest College and University Associated for Sciences (Washington State University) under Grant DEFG06-89ER-75522 with the U.S. Department of Energy.

This investigation was partially supported by the Faculty Research Fund of Central Washington University, Ellensburg, Washington 98926.

The Pacific Northwest Laboratory is operated for the U.S. Department of Energy by Battelle Memorial Institute under Contract DE-AC06-76RLO 1830.

NOMENCLATURE

A	fiber cross sectional area, in^2
A_p	fiber projected area, in^2
M	modulus of elasticity of quartz fiber, psi
C_L	lift coefficient, dimensionless
C_n	constants for the bending moment equation
D	fiber diameter, in
F_L	fiber lift force, lbs
f	functional notation
f_n	fiber natural frequency, Hz
f_s	vortex shedding frequency, Hz
g	gravitational constant, ft-lbm/lbf-sec^2
I	moment of inertia of circular fiber cross section, in^4
k	P/(E)(I), $1/in^2$
L	fiber length equal to pipe inside diameter, in
M_{max}	maximum bending moment in stretched fiber, lb-in
N	number of waves of phase change, dimensionless
n	index of refraction, dimensionless
P	induced axial force on fiber due to bending load, lb
P_o	fiber axial pre-tension load, lb
Re_D	Reynolds Number based on diameter, in
S	Strouhal Number, dimensionless
t	time, sec
V	average flow velocity, ft/sec
w	unit loading on fiber, lb/in
y_{max}	maximum deflection at center span of stretched fiber, in
ϵ_A	axial strain in fiber, in/in
μ	absolute viscosity
ρ	air density, lb/ft^3
ρ_F	mass density of fiber, lb/in^3
$\Delta\Phi$	phase change of light due to axial fiber strain, radians
ω	angular frequency, rad/sec
σ_{max}	maximum tensile stress, psi
λ	wavelength, nm

INTRODUCTION

The work discussed in this paper pertains to a flow measurement concept based on a fiber optic interferometric technique. The idea for the project was first conceived at the Pacific Northwest Laboratory (PNL), operated by Battelle Memorial Institute in Richland, Washington, as a result of their desire for a new and innovative gas flow measuring technique having inherently high accuracy.

Exploratory research on the project was funded by a grant from the U.S. Department of Energy and was conducted by the author at PNL during the summer of 1990 while employed as a Northwest College and University Association for Science (NORCUS) Faculty Research Appointee. By the end of the summer appointment, feasibility of the concept was established, and permission was given to continue the investigation on the campus of Central Washington University (CWU) in Ellensburg, Washington. CWU also contributed funding to purchase some test equipment that was not available from PNL.

The operation of the fiber optic flow sensor is based upon the well-established principle of vortex shedding behind a cylinder in cross-flow. A fiber is stretched across a pipe which contains a flowing gas, and the resulting cross-flow induces a time-varying force as shown in Fig. 1. The force produces an axial strain in the sensing fiber, which in turn causes a time varying change in laser beam intensity, sensed by a detector. The time-varying signal contains a frequency component which is called the vortex shedding frequency and is proportional to velocity. Since the fiber is stretched across the pipe, the fiber integrates the velocity profile and yields a velocity that is proportional to the volume flow rate. The detection scheme uses interferometry as a means of generating the flow-rate induced signal. As shown in Fig. 2, a Mach-Zehnder interferometer (Krohn, 1988) is employed. Interferometry provides an extremely sensitive measurement with potential for high accuracy.

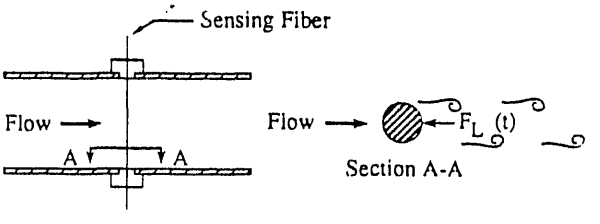

Fig. 1 Fiber Structure for Measurement of Gas Flow

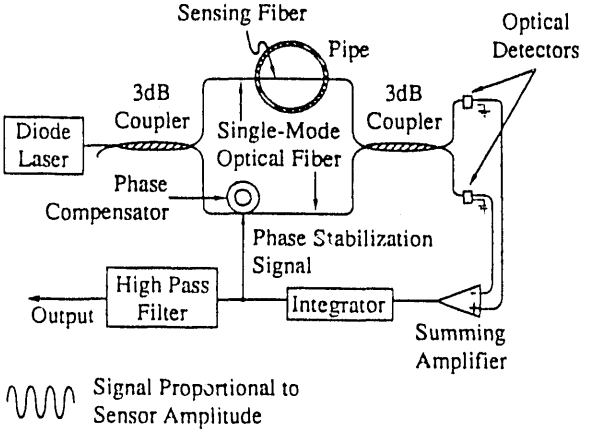

Fig. 2 Fiber Optic Mach-Zehnder Interferometer Design

The analytical and experimental study was limited to gas velocities ranging from 5 to 50 ft/sec based upon potential applications. The instrument has the capability of sensing velocities beyond 50 ft/sec, but there is a lower limit dictated by a diameteral Reynolds Number of about 50 where the vortex shedding effect is not observed.

The project proceeded along three paths of investigation:

1. Analytical, utilizing a simple first order model.
2. An experimental investigation utilizing helium-neon wavelength fibers to study the basic principles involved in fiber interferometry and signal processing.
3. An experimental investigation utilizing an 830 nm diode laser system and low loss (3 db) fiber couplers. These tests were intended to quickly assess the feasibility of the fiber flow sensing concept and point to future work.

FIRST ORDER ANALYSIS

As an aid in developing the design concepts and establishing an experimental program, a simplified first order analysis was performed. The following assumptions were made.

Flow:

1. The flowing medium is air at 1 atm. and 75 deg. F.
2. Constant properties are considered (density and viscosity).
3. The flow is steady in time.
4. The Strouhal Number describes the flow-induced, time-varying force input into the fiber optic.

Fiber Optic:

1. Fused quartz material properties: E = 10.15×10^6 psi, density = 137.4 lb/cu.ft
2. Single mode fiber, wavelength, λ = 632.8 nm and 830 nm.
3. Fiber optic property: n = 1.458, P_{12} = 0.27 (Pockels coefficient)

Fiber Optic Mechanics:

1. Built-in walls are assumed that induce an axial force component in the fiber.
2. String behavior, i.e., there is a slope at the wall but there is no vertical deflection.
3. Spatially uniform loading (w, lb/in.) caused by the alternating lift force. The lift force is calculated on the basis of a flow averaged velocity.

Mathematical Model

The major features of the mathematical model are summarized below. Fig. 3a shows a cylinder in cross-flow with the vortex pattern emerging in its wake. Experiments show that the oscillations in lift force (force perpendicular to the flow) occur at the shedding frequency, but oscillations in the drag force (force parallel to the flow) occur at twice the shedding frequency (Blevins, 1990). Since it is the vortex shedding frequency that is of interest here, Eq. 1 is used to predict the time-varying lift force. The drag force component was ignored in this first order analysis. The Strouhal Number, S, is given in Fig. 4 as a function of diameteral Reynolds Number.

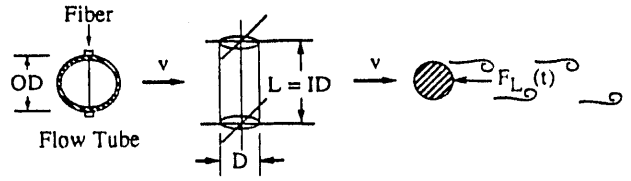

(a) Fluid dynamic model.

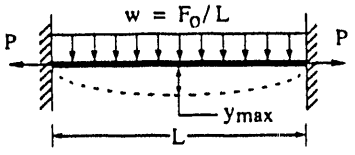

(b) Stress / deflection model.

Fig. 3 Mathematical Modeling of a Stretched Fiber

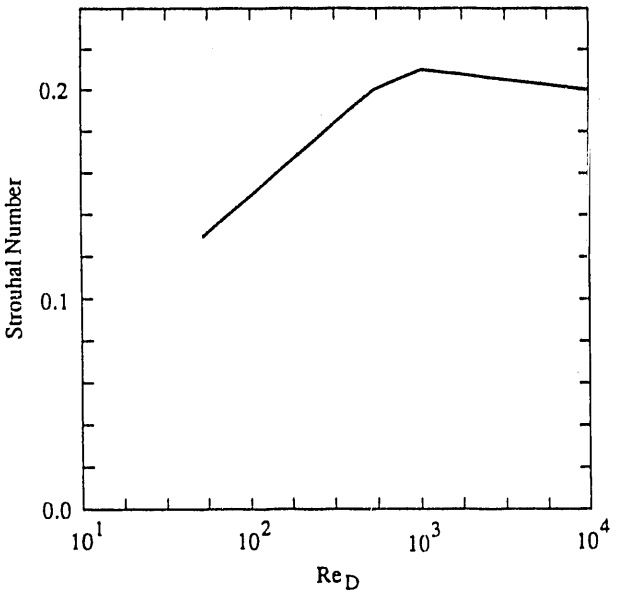

Fig. 4 Strouhal Number Variation with Diameteral Reynolds Number

$$F_L = C_L [\rho V^2/2g] A_p \sin \omega t \quad (1)$$

where

$C_L = 1.0$

$A_p = LD$

$\omega = 2\pi f_s$

$f_s = S(V/D)$

$S = f(Re_D)$

A schematic representation of the stress/deflection model is given in figure 3b. Roark's Formulas for Stress and Strain (Young, 1989) applies to this situation. Eq. 2 gives the maximum vertical displacement of the center of the fiber and Eq. 3 gives the induced axial force due to the bending load. The maximum bending moment is given by Eq. 4 with the constants defined below.

$$y_{max} = L\left[\frac{3wL}{64EA}\right]^{1/3} \quad (2)$$

$$P = wL^2/8y_{max} \quad (3)$$

$$M_{max} = -\frac{w}{k^2}\left[\frac{C_4^2 - C_3 C_{a5}}{C_3^2 - C_2 C_4}\right] \quad (4)$$

where:

$C_2 = \sinh(kL)$

$C_3 = \cosh(kL - 1)$

$C_4 = C_2 - kL$

$C_{a5} = C_3 - (P/2EI)L^2$

The maximum stress in the fiber due to bending, induced axial loading, and pre-tension is given in Eq. 5.

$$\sigma_{max} = P/A + P_o/A + |M_{max}|\, D/2I \quad (5)$$

The axial strain induced by the axial, time varying force P is given by Eq. 6.

$$\epsilon_z = P/AE \quad (6)$$

The resulting phase change due to the axial strain is given by Eq. 7 in terms of radian units and by Eq. 8 in wave number units.

$$\Delta\Phi = \epsilon_z\, [1 - (n^2 P_{12})/2](2\pi n L)/\lambda \quad (7)$$

$$N = \Delta\Phi/2\pi \quad (8)$$

Finally, the natural frequency of the optical fiber is given by Eq. 9.

$$f_n = \frac{1}{2L}\sqrt{\frac{Pg}{w + \rho_F A}} \quad (9)$$

Using the above model, a parametric study was conducted for the purpose of developing design concepts as well as making performance predictions to aid in interpreting experimental results. The variables that were investigated in the design study were flow velocity, fiber length, fiber diameter, and fiber preload.

Fig. 5 shows the variation of phase change in both radian and wave units as flow velocity is varied from 0 to 50 ft/sec. It is apparent that the fraction of a wavelength must be measured. Fig. 6 shows the effect of increasing the sensing fiber's length with all other parameters held fixed (as in Fig. 5). When the sensing fiber length is doubled, the sensitivity or phase change increases by a factor of three and numerically becomes greater than one wave above 35 ft/sec. Fig. 7 shows the effect of increasing fiber preload from 0 to 2 lbs on vortex shedding frequency and natural frequency as well as on fiber tensile stress for a fixed flow velocity of 40 ft/sec. The results clearly show

that the natural frequency and vortex shedding frequency can be matched at best at only one value. This point will be discussed in a later section dealing with the triple strand sensor. At 2.0 lbs pretension, the tensile stress in the fiber approaches 27,000 psi which is a little over one-half of the proof stress for a 125 micron fiber having a 250 micron cladding diameter. A proof stress of 50,000 psi was quoted by a fiber manufacturer. The proof stress would be reached if the fiber were preloaded to 3.6 lbs.

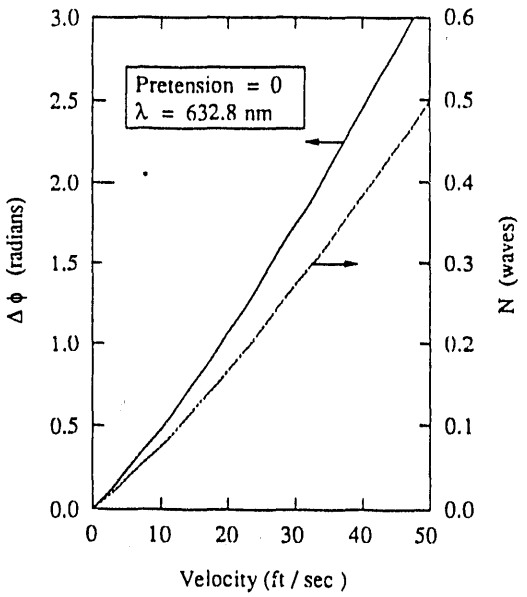

Fig. 5 Sensitivity of Fiber Optic Flow Sensor as a Function of Flow Velocity

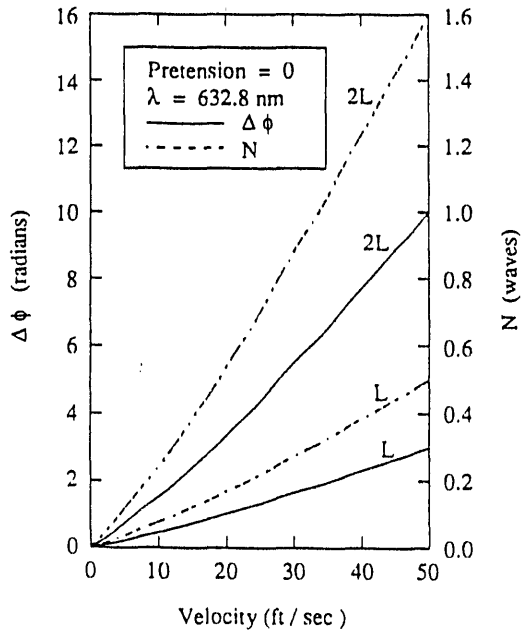

Fig. 6 Effect of Changing Fiber Sensor Length on Sensitivity

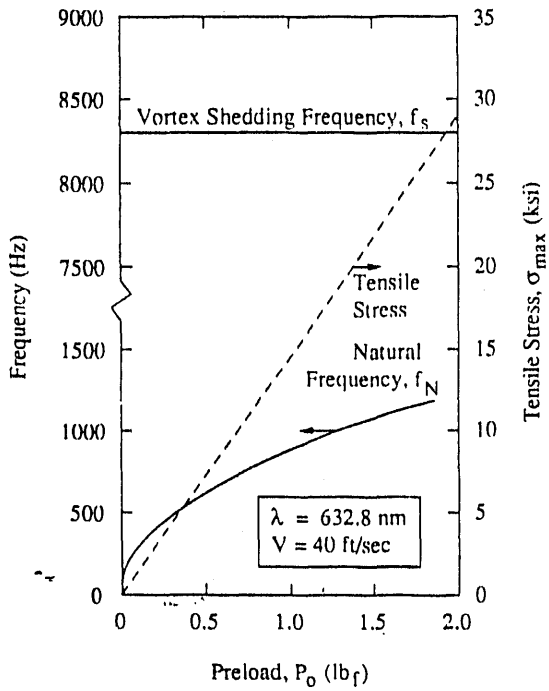

Fig. 7 Variation of Natural Frequency, Vortex Shedding Frequency, and Fiber Tensile Stress with Fiber Preload

Table 1 shows the effect of varying fiber outer diameter from .00984 in. (250 microns) to .080 in. on fiber stress, signal (vortex shedding frequency), phase change and natural frequency. Fibers with diameters greater than .060 in. would cause problems in signal acquisition since the phase change would be less than one-tenth of a wave. The flow velocity was held fixed at 40 ft/sec. and the pre-tension was 2.0 lbs.

Table 1. Effect of Varying Fiber Diameter

Diameter (in.)	Tensile Stress (psi)	Shedding Frequency (Hertz)	ΔΦ (radians)	N (waves)	Natural Frequency (Hertz)
0.00984	26,510	8,239	2.448	0.390	1272
0.020	6,447	4,080	1.366	0.217	946
0.040	1,635	2,040	0.861	0.137	646
0.060	739	1,360	0.657	0.105	511
0.080	423	1,020	0.542	0.086	431

EXPERIMENTS WITH HELIUM-NEON WAVELENGTH FIBERS

Fig. 8 shows a schematic representation of the optical table setup for the initial experiments at the He-Ne wavelength. The purpose of this testing was to obtain experience in making a fiber interferometer and obtaining preliminary information and experience in acquiring and interpreting signals from the detector which in this case was an S20, extended IR photomultiplier tube. The fiber lengths utilized were 1.0 meter in length. Approximately 1.0 mW of laser power was transmitted per fiber channel. The two fibers were placed

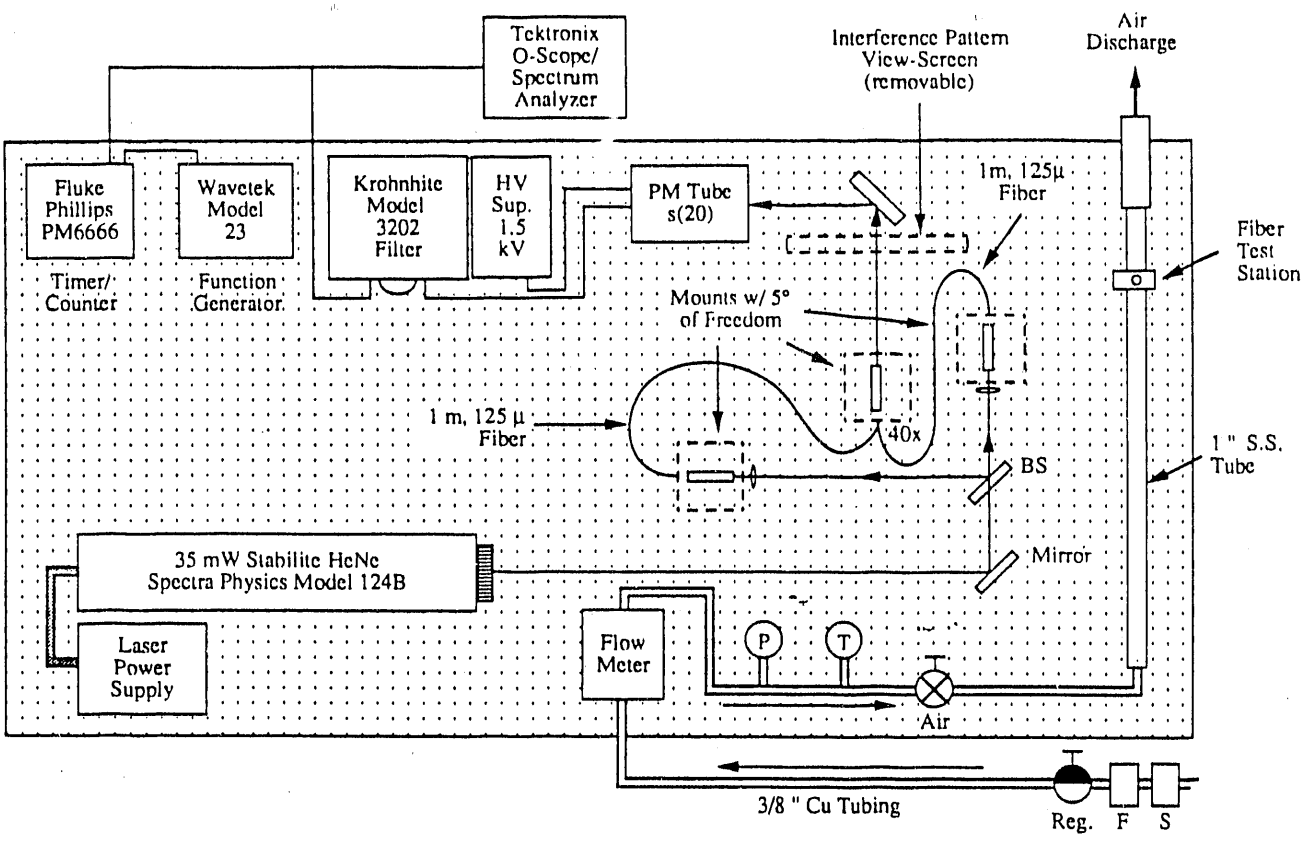

Fig. 8 Schematic of Initial HeNe Wavelength Experimental Setup

side by side in contact with one another and expanded through a microscope objective lens. The interference pattern observed was of good contrast with excellent fringe visibility. Thermal drift was observed by studying the interference pattern both by eye as well as with a detector. Thermal drift was measured to have 2 to 6 waves of phase shift at frequencies from 1 to 12 Hz. In another experiment, with a fiber stretched at a spacing of approximately 1.0 in., weights were placed at mid span to determine static deflection of the fiber and its corresponding phase shift. The measured phase shifts corresponded well to predicted values.

A flow system was designed to provide suitable test conditions using air as the medium. Fig. 8 shows the components used. A flow tube was designed to produce a fully developed turbulent velocity profile at 40 ft/sec. The tube is 40 in. long with an inside diameter of 0.88 in. giving a pipe Reynolds Number of 17,160. Fig. 9 shows a photograph of the fiber test section which allows the fiber to be positioned transverse to the flow when mounted in Conax fittings.

Initial testing of a single HeNe fiber stretched across the test section contained signals that were corrupted by both thermal and acoustic signals. The acoustic signal components were identified by using a small Knowles Electronics, Inc., microphone probe (Model 1834 EW 192). The acoustic noise signals encompassed a spectrum from 100 to 5,000 Hz with high amplitudes at 100, 2500, and 6000 Hz. The major noise source was identified to occur at the exit of the test section (originally operated as a free jet) and at the entrance where a 0.375 in. tube joined the 1.0 in. diameter tube. These noise sources were eliminated by reworking the test flow tube with the addition of a large diameter muffler with sound-absorbing material at the discharge and by adding a plenum to the entrance which also includes sound-absorbing material.

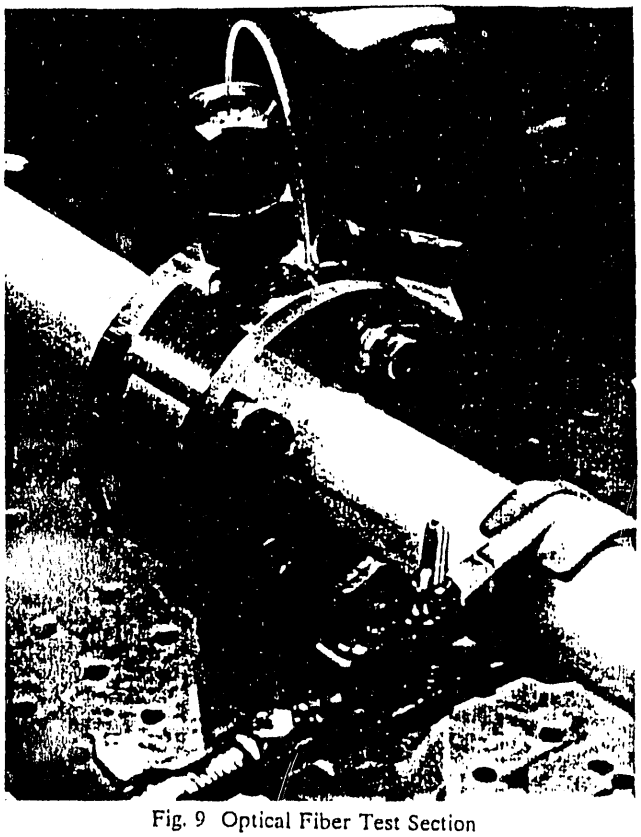

Fig. 9 Optical Fiber Test Section

The acoustic noise was reduced by several orders of magnitude. At this point, it was found that the vortex shedding frequency signals were of the same order of magnitude as the residual acoustic signals. Work continued after changing over to the 830 nm laser diode system.

EXPERIMENTS WITH 830 NANOMETER WAVELENGTH FIBERS

A Mach-Zehnder interferometer was set up as shown in Fig. 2 with the exception of the phase stabilization loop (compensator and integrator). The signals were measured using two EG&G Model UV-444BQ silicon detectors. The two channels of signals were combined using an Ithaco, Model 1201, Low Noise Preamplifier. The signals were analyzed on a Hewlett Packard Model 4195A Spectrum Analyzer.

Four different fiber sensing configurations were tested to date as shown in Fig. 10. The first case consisted of a single strand of mono-mode fiber that was stretched across the flow stream. The second configuration consisted of three strands of fibers arranged side by side which presented a larger cross section to the flow. The third configuration involved two strands of mono-mode fibers that were stretched in line across the flow stream. The last design was an attempt to package the sensing and reference fibers into a tubular probe configuration.

Initial testing of the single fiber sensing element at 830 nm in an air flow test section showed signals that were corrupted by acoustic and thermal noise as observed earlier with the HeNe wavelength interferometer.

Lyle and Pitt (1981) reported on a similar fiber optic flow sensor. The experiment was conducted in water and used a multimode fiber, relying on speckle interferometry for phase information. Subsequent modeling of their system revealed that the sensor had about eight times the force exerted on the fiber at lower velocities than the airflow testing of the subject experiments. However, the most significant difference is that the vortex shedding frequencies in the referenced paper were much lower than corresponding frequencies associated with the airflow of this work. Reviewing the referenced work produced the idea of trying to mimic their performance regime, but for air flow conditions. Fig. 11 shows design details of a triple fiber sensor design. Three fiber lengths were bonded together to form a structure that was three times wider than its thickness. The fibers were aligned with their widest dimension perpendicular to the flow. Epoxy was carefully smeared over the fibers. Dimensional inspection of the fiber showed the sensor to be .0354 in. wide and .0118 in. thick. Both sensor and reference fibers measured 78.625 in. ±.08 in. in length. The chosen geometry down shifts the vortex shedding frequencies into the range 500 Hz to 2500 Hz instead of 1500 Hz to 11,000 Hz as previously tested for a single fiber. From a structural standpoint, the three fibers generate a greater drag and lift load; and since the fibers are optically three times longer, the sensitivity in terms of phase change should increase significantly. Fig. 12 shows predicted performance of the fiber optic flow sensor in terms of natural frequency, vortex shedding frequency, and flow velocity. Also shown on the graph of Fig. 12 are measured data points taken on three separate days. The analysis and the confirming data indicate the following:

1. The frequency is indeed shifted down.
2. Although there is a more-than-desired spread in data, the data follows the linear variation with velocity as predicted.
3. There is a crossing between the shedding frequency and natural frequency at about 1500 Hz. Signals were difficult to detect in this regime, an effect also observed in the referenced work.
4. The signal sensitivity increased in terms of phase change.

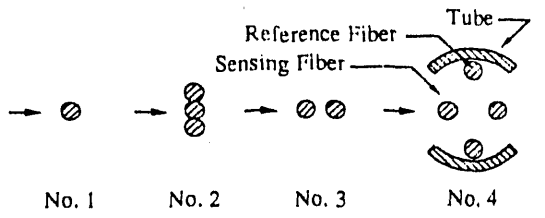

Fig. 10 Sensing Fiber Configurations Tested

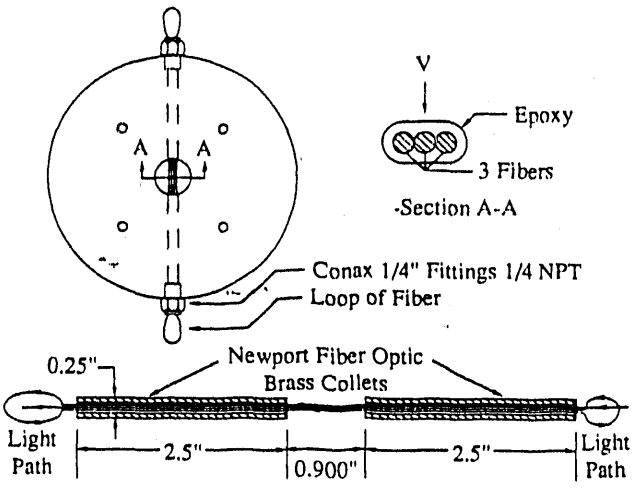

Fig. 11 Triple Fiber Sensor Design

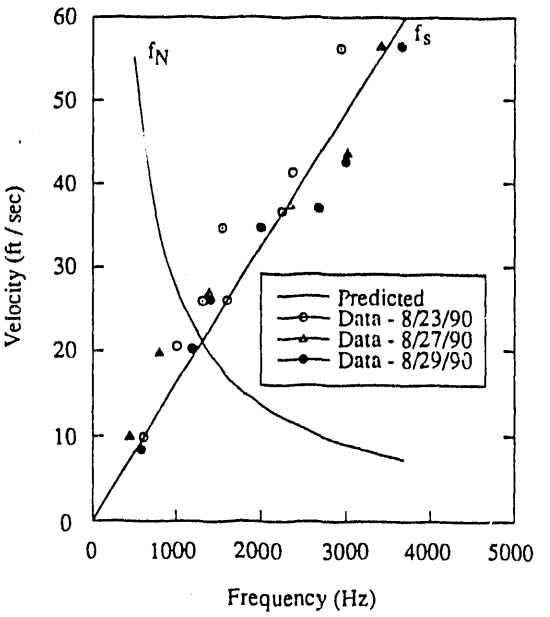

Fig. 12 Experimental Results from Triple Strand Fiber Sensor Crossplotted Against Predicted Performance, λ = 830 nm

Fig. 10, configuration number 3, shows another arrangement of the fiber flow sensor. It is referred to as a twin fiber sensor. Two fibers are held apart by plugs with a spacing of .120 in., span the test section. In this design each fiber acts independently as far as responding to flow forces, but they are connected optically (twice the optical path). Two variations are possible. One of the options is to orient both fibers perpendicular to the flow and the other variation has one fiber positioned behind the other in the flow. Testing has shown that when fibers are oriented perpendicular to the flow, no signal is observed because it is suspected that each fiber experiences slightly different flow disturbances and destroys any meaningful phase relationship. The second fiber orientation did produce good results as shown in Fig. 13. Fig. 13 shows two sets of data plotted on a predicted curve of vortex shedding frequency versus velocity. In this configuration, the performance matches single fiber predictions.

The last configuration to be tested was configuration number 4 as shown in Fig. 10. The idea behind this design was an attempt to null out the acoustic noise effects by exposing the reference fiber to the exact same noise field as the sensor fiber. This was accomplished by lightly epoxying the reference fiber to the probe side wall, such that response to flow was not possible. The net expected result was that only vortex shedding frequencies would be observed (thermal effects are also reduced).

Fig. 14 shows the results of a single set of test data obtained with this configuration. Although the data appear to follow the predicted curve reasonably well, the frequency signals were not as clean nor unambiguous as hoped for. One possible explanation for this result was that too much epoxy surrounded the reference fibers and prevented the fibers from responding to the acoustic pressure waves.

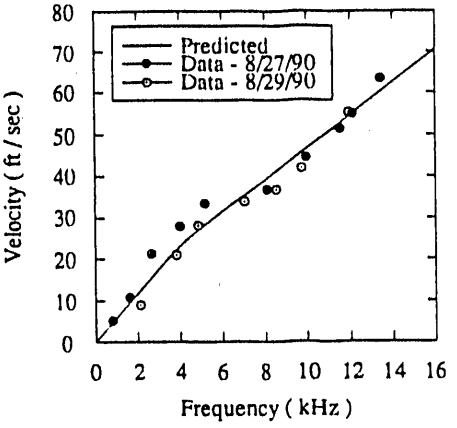

Fig. 13 Experimental Results from Twin Fiber Sensor Crossplotted Against Predicted Performance

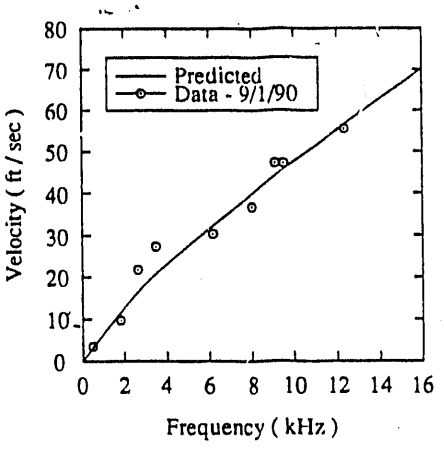

Fig. 14 Experimental Results from a Twin Fiber Probe Crossplotted Against Predicted Performance

CONCLUSIONS

Preliminary experimental results indicate the feasibility of a laser fiber optic sensor for gas flows. Acoustic noise is present in all gas flows and must be dealt with in an effective manner if the subject flow measuring concept is to become a reality. Several possible solutions are suggested below:

1. Separate the desired vortex shedding frequency from the acoustic noise spectrum by either up or down shifting.
2. Sense the acoustic noise and subtract using signal processing techniques.
3. Investigate the possibility of using a different type of interferometer such as a Fabry-Perot.

Testing to date has shown that the use of a modulator in the reference arm of the interferometer will be required.

Preliminary tests with a triple fiber, which presents a wider body in cross-flow, produced the expected and desired result of down shifting the vortex shedding frequencies to lower values. Frequencies in the 500 to 3000 Hz range were measured. This direction of testing should be continued with even wider fiber configurations.

In order to have a fiber sensor that is durable, it must be configured in probe form and be insertable. Preliminary results with a probe configuration has shown promise even though the results did not meet all objectives, such as minimizing acoustic noise.

ACKNOWLEDGEMENTS

The authors would like to thank Dr. Jimmie R. Applegate, Dean, School of Professional Studies, and Dr. Robert M. Envick, Chairman, Department of Industrial and Engineering Technology at Central Washington University for their encouragement and support. The authors would also like to acknowledge the help and discussions so freely given by Mr. Kurt Stahl and Dr. Karl Davis of the Pacific Northwest Laboratory.

REFERENCES

Blevins, R. D., Flow-Induced Vibration, 2nd Edition, Van Nostrand Reinhold, New York, 1990, pp. 47 and 61-63.

Krohn, D. A., Fiber Optic Sensors, Instrument Society of America, 1988, pp. 45-46 and 52-55.

Lyle. J. H., and C. W. Pitt, "Vortex Shedding Fluid Flowmeter using Optical Fibre Sensor," Electronic Letters, Vol. 17, No. 6, 1981, pp. 244-245.

Young, W. C., Roark's Formulas for Stress and Strain, 6th Edition, McGraw-Hill Book Co., New York, 1989, p. 179, Case 6, Table 12.

END

DATE FILMED

3/16/92